

Inductively-Powered Direct-Coupled 64-Channel Chopper-Stabilized Epilepsy-Responsive Neurostimulator with Digital Offset Cancellation and Tri-Band Radio

Hossein Kassiri¹, Arezu Bagheri², Nima Soltani¹, Karim Abdelhalim³, Hamed Mazhab Jafari², M. Tariqus Salam^{1,4}, Jose Luis Perez Velazquez⁴, Roman Genov¹

¹ Department of Electrical and Computer Engineering, University of Toronto, Canada; Email: hkassiri@eecg.utoronto.ca

² Semtech Inc., Toronto, ON, Canada. ³ Broadcom Inc. Irvine, CA, USA

⁴ Brain and Behavior Programme and Division of Neurology, Hospital for Sick Children, University of Toronto, Canada

Abstract—An inductively powered 0.13 μm CMOS neurostimulator SoC for intractable epilepsy treatment is presented. Digital offset cancellation yields a compact 0.018mm² DC-coupled neural recording front-end. Input chopper stabilization is performed on all 64 channels resulting in a 4.2 μV_{rms} input-referred noise. A tri-band FSK/UWB radio provides a versatile transcutaneous interface. The inductive powering system includes a 20mm x 20mm 8-layer flexible receiver coil with 40% power transfer efficiency. In-vivo chronic epilepsy treatment experimental results show an average sensitivity and specificity of seizure detection of 87% and 95%, respectively, with over 76% of all seizures aborted.

I. INTRODUCTION

Closed-loop neurostimulation, triggered by accurate epileptic seizure detection, has been shown promising in reducing seizure frequency in intractable epilepsy patients and in epilepsy animal models [1]. Today, there is an effort to perform monitoring, detection and treatment of various neurological disorders using a fully-implantable SoC. A system for such responsive neurostimulation with high treatment efficacy requires low-noise compact-channel multi-site neural recording, low-power on-chip time-advanced seizure detection, versatile wireless diagnostic data communication, and power and configuration telemetry. There are several integrated neural interfaces reported in the literature [2]–[6], that are designed and implemented to record neural signals and in some cases [2]–[4], trigger stimulation upon detection of an event. However, there are only a few systems in the literature such as [2], [3] that demonstrate a complete closed-loop solution capable of on-chip monitoring, signal processing and closed-loop treatment. In addition, to move toward the goal of a fully implantable system, wireless data communication and power telemetry are required for such neurostimulators.

We present a 16mm² wireless 0.13 μm CMOS SoC with 64 DC-coupled chopper-stabilized digitally-calibrated neural recording and stimulation channels. The chip benefits from a quad-core DSP for on-chip seizure detection and three wireless transmitters for data communications in different frequency bands. Power and configuration commands are provided through an inductive link, which makes the electrodes to be the only wires required to be connected to the chip.

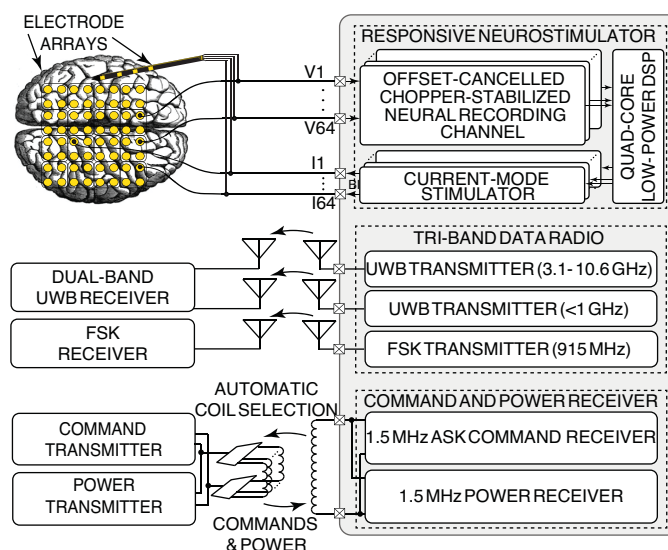


Fig. 1. A simplified functional diagram of the neurostimulator SoC and peripheral blocks.

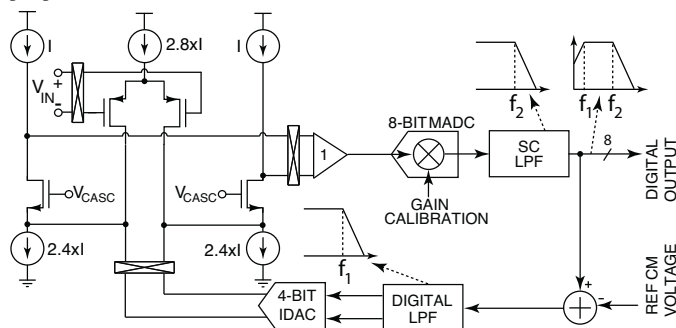


Fig. 2. DC-coupled chopper-stabilized neural recording channel with digital calibration.

II. SYSTEM ARCHITECTURE

Fig. 1 depicts the system architecture of the responsive neurostimulator SoC. It includes 64 chopper-stabilized recording channels, a quad-core low-power DSP, 64 current-mode neurostimulators, a triple-band RF transmitter, and an inductive command and power receiver. Large input DC blocking

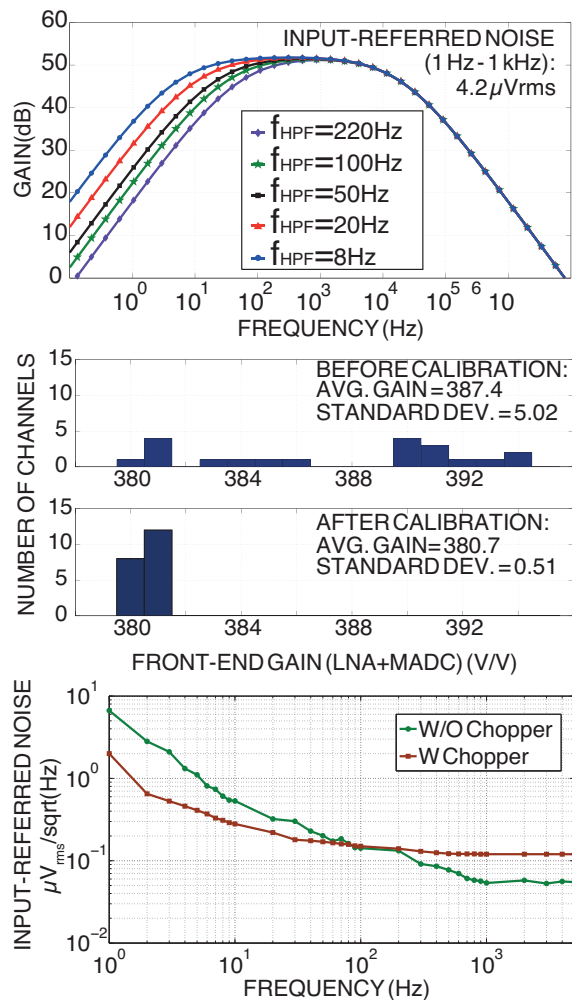


Fig. 3. Experimentally measured: amplitude response of the front-end with adjustable HPF pole (top), online gain mismatch calibration using MADC (middle), input-referred noise with and without chopper stabilization (bottom).

capacitors in the recording channels are eliminated yielding a compact front-end implementation. The DSP computes the first derivative of the neural signals synchrony (i.e., spatial neural synchrony fluctuations), 16 channels per core. Once an advanced detection of an epileptic seizure is made, a biphasic current-mode stimulation pulse train is applied to a subset of the stimulation electrodes with a spatio-temporal profile specifically chosen for a given subject (a rodent or a human patient). The recorded EEG data and status signals are transmitted out transcutaneously by a triple-band RF radio. The under-1GHz UWB short-range (10cm) transmitter communicates to an on-skin wearable receiver. The 3.1-10.6GHz UWB mid-range (1m) transmitter communicates to a handheld receiver. The 915MHz FSK long-range (10m) transmitter communicates to an indoor stationary receiver. Energy is transmitted by a single coil through a multi-coil cellular inductive link at 1.5MHz frequency. The power receiver outputs 30mW maximum power for the 12cm transmission distance with power efficiency of 40 percent. An ASK-demodulating command receiver reuses the same inductive link to recover transmitted commands and the clock.

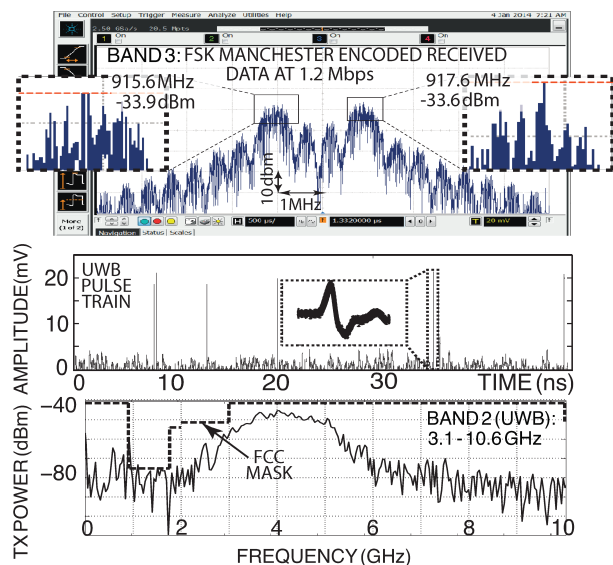


Fig. 4. Experimentally measured spectrum of FSK (top) and UWB (bottom) pulse-train generated by on-chip transmitters.

III. CIRCUIT IMPLEMENTATION

The neural recording channel is shown in Fig. 2. The channel includes a fully differential low-noise folded-cascode OTA, an 8-bit multiplying SAR ADC, a switched-capacitor LPF, a digital integrator, a digital delta-sigma modulator, and a 4-bit offset-canceling DAC. Instead of using conventional large input DC blocking capacitors, digitally-assisted input offset cancellation is employed to enable DC input coupling [7]. The digital integrator in the feedback implements a low-cut-off-frequency LPF. The resolution of the integrator output signal is reduced to 4 bits by the delta-sigma modulator. The resulting 4-bit low-pass-filtered signal is subtracted from the input signal by means of the 4-bit current-steering DAC connected to the OTA folding nodes. This effectively implements an HPF with a digitally programmable low cutoff frequency (e.g., 1Hz) and cancels out the DC offset in the input signal (up to ± 50 mV). The digitally programmable switched-capacitor LPF in the feed-forward path sets the stop frequency of the resulting BPF pass band. The BPF frequency corners are thus well-controlled and insensitive to mismatch and PVT variations. The integration area is reduced by 80 percent compared with an equivalent AC-coupled implementation [3]. Additionally, DC input coupling allows for direct input signal chopping without the overhead of large noise multiplication compensating capacitors, an input impedance compensation loop, and a ripple compensation loop. The BPF pass band channel-to-channel gain mismatch inherent to such an open-loop implementation is calibrated online by the multiplying ADC which scales the digital output by a programmable coefficient.

IV. EXPERIMENTAL RESULTS

Fig. 3 (top) shows the amplitude response of the front-end for HPF pole frequency from 1Hz to 1kHz, adjusted using the digital coefficient λ . Larger values of λ reduce the cut-off frequency to below 1Hz. The BPF pass band channel-to-channel gain mismatch inherent to such an open-loop OTA

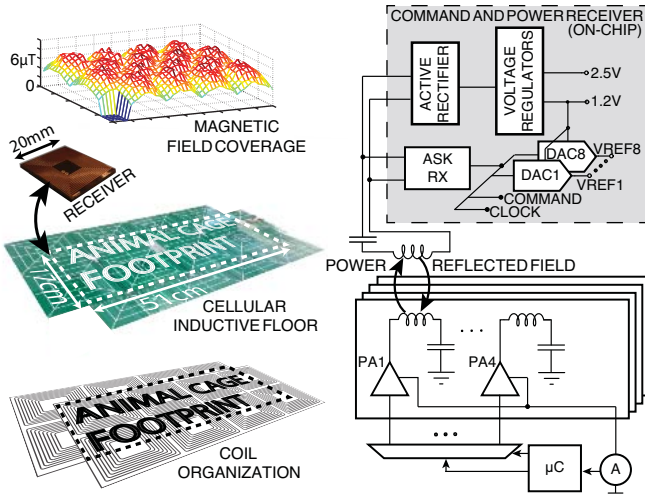


Fig. 5. Cellular inductive powering system.

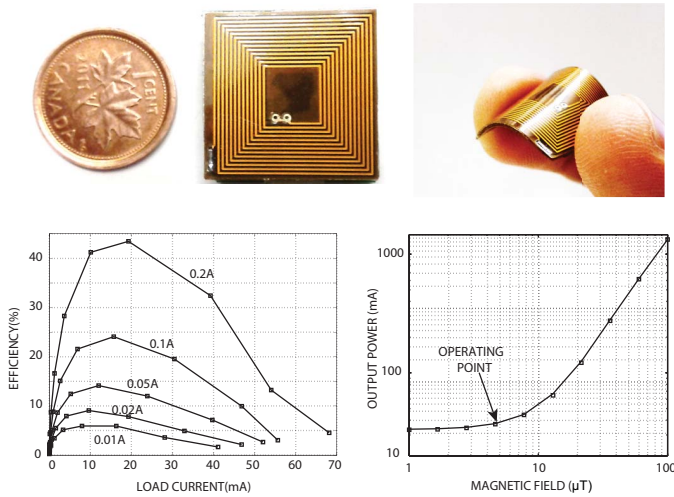


Fig. 6. Experimentally measured power transfer efficiency and sensitivity.

implementation is calibrated online by the multiplying SAR ADC (MADC in Fig. 2), which scales the digital output down by a programmable coefficient (Fig.3, middle). The experimentally measured input-referred noise integrated from 1Hz to 1kHz is $7.5\mu\text{V}_{\text{rms}}$ without chopping, and $4.2\mu\text{V}_{\text{rms}}$ with chopping (Fig. 3, bottom). Fig. 4 (top) shows experimentally measured spectrum of 1.2Mbps Manchester-encoded pulse train generated by the FSK transmitter centered at 916.4MHz, and Fig.4 (bottom) shows a 54Mbps pulse train generated by a UWB transmitter and its spectrum plotted over FCC mask for indoor applications.

For freely moving rodent epilepsy studies, the neurostimulator is powered by an inductive powering system shown in Fig. 5 (left, middle and bottom). It consists of a two-layer network of 16 planar high-Q ($Q=129$ for 4 ounce copper trace) inductive coils placed under a non-conductive rat cage floor and acting as an energy transmitter, and a small multi-layer flexible coil which is the receiver. The transmit coils are arranged in two 2×4 arrays of PCB coils placed on top of one another as depicted in Fig. 4 (left, bottom). The

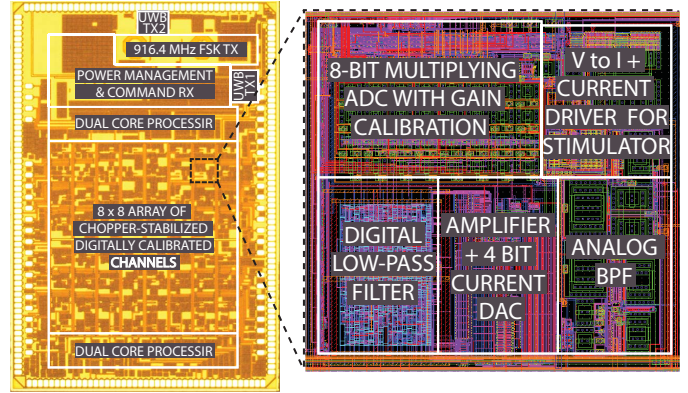


Fig. 7. Micrograph of the 16mm^2 SoC (left) and layout of 0.09mm^2 recording and stimulation channel (right).

arrays are offset by 50 percent of the coil pitch in both x and y dimensions to eliminate magnetic field dead zones. To maintain the low specific absorption rate requirement, only the coil nearest to the receiver, is selected by a microcontroller sensing the current in the power amplifiers (PA) supply line induced by the secondary magnetic field (reflected by the receiver) (Fig. 5 (right)). The voltage induced on the LC-tank is then rectified. Two voltage regulators generate 1.2V and 2.5V supply voltages. An 8-channel 8-bit DAC generates additional eight voltage levels from 0V to 1.2V for biasing and reference nodes. As shown in Fig. 5 (top, left), the experimentally measured intensity of the magnetic field at the nominal distance of 12cm above the floor is within 13% of the nominal value of $6\mu\text{T}$.

The receiver coil (Fig. 6, top, right and left), is a $20\text{mm} \times 20\text{mm}$ stack of four flexible two-layer PCBs for a total of eight layers. It is placed on the top of the neurostimulator package. The flexibility allows to tailor-fit the coil to the shape of the implantation site (e.g., the curvature of a rat scalp). The stacked coil configuration achieves a high quality factor of 24 despite the small size and results in a better overall wireless power transfer efficiency of over 40%. Fig. 6 (bottom, left) shows experimentally measured power transfer efficiency for various currents consumed by the load. The ideal loading condition is when the system consumes approximately 15mA, at which point the input impedance of the active rectifier is matched to the output impedance of the receiver coil. Fig. 6 (bottom, right) depicts the power received at different intensities of the magnetic field at the receiver. Due to the significantly increased quality factor, the stacked configuration results in more power harvested from the transmitted magnetic field as compared to a conventional single-layer coil, for the same field intensity.

The micrograph of the $4.85\text{mm} \times 3.3\text{mm}$ SoC implemented in a standard 1P8M $0.13\mu\text{m}$ CMOS technology is shown in Fig. 7(left). The layout of the channel including the neural chopper-stabilized amplifier, digitally programmable low-pass filter, biphasic current driver, SAR multiplying ADC, and 4-bit current steering DAC is depicted in Fig. 7(right).

The SoC was validated in a 500-hour chronic treatment of temporal lobe epilepsy (rat model). Four Wistar rats were

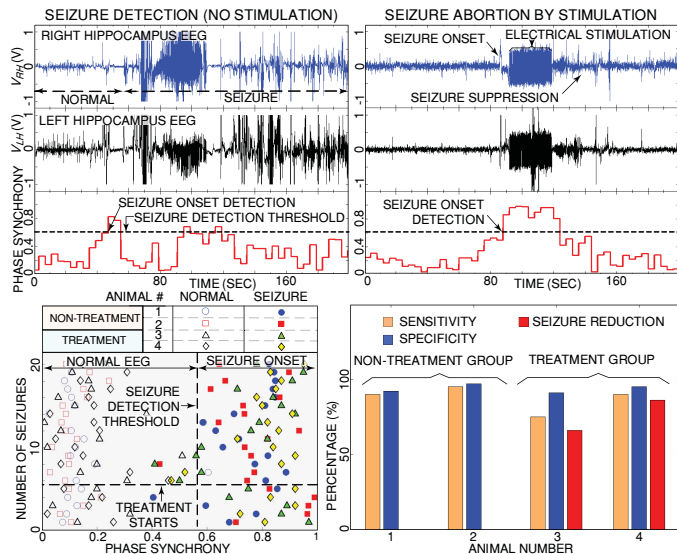


Fig. 8. In-vivo seizure detection and closed-loop stimulation results.

intraperitoneally injected kainic acid which induced recurrent spontaneous motor seizures within one to two months. The rats underwent craniotomy for hippocampus microelectrodes implantation and were divided into two equal groups: the non-treatment group and the treatment group. In each rat, the electrodes were connected to the presented SoC for automatic seizure detection. Each rat was also video monitored for seizure labeling. Fig. 8 (top, left) shows an example of in-vivo on-line real-time seizure detection in the non-treatment group. In the treatment group the SoC was also configured to automatically trigger the closed-loop electrical stimulation for the purpose of suppressing upcoming seizures. Fig. 8 (top, right) illustrates the SoC-triggered stimulation upon a seizure onset detection in the treatment group. Fig. 8 (bottom, left) demonstrates the seizure onset detection performance. The average sensitivity and specificity of the detection are 87% and 95%, respectively. Seizure frequency has been reduced on average by over 76% in the treatment group compared to the non-treatment group, as shown in Fig. 8 (bottom, right).

A comparative analysis is given in Table I where this work demonstrates advanced functionality among recently published state-of-the-art neural interface SoCs.

V. CONCLUSION

A 0.13 μm CMOS wireless closed-loop neural interface SoC is presented. The SoC has 64 direct-coupled chopper-stabilized recording channels with digital calibration and offset removal. An on-chip quad-core DSP is implemented for epilepsy seizure detection using derivative of phase synchrony. Upon detection, the DSP triggers an arbitrary subset of 64 on-chip stimulators for seizure abortion. The chip also benefits from a tri-band wireless transmitter for versatile transcutaneous interface and a flexible 8-layer coil for wireless power and command reception. Total power dissipation is 5.78mW and 2.17mW with and without FSK transmitter respectively. The system is characterized in-vivo in a 500-hour chronic treatment of a rat

TABLE I
STATE-OF-THE-ART NEURAL RECORDING AND/OR STIMULATION SOCS

Spec.	[3]	[5]	[2]	[8]	THIS WORK
Tech. (μm)	0.13	0.5	0.18	0.065	0.13
Area (mm^2)	12	16.4	13.47	5.76	16
Supply (V)	1.2	3	1.8	0.5	1.2/2.5
Power (mW)	1.5	7.05	2.8	0.225	2.17-5.8*
# Record Chan.	64	32	8	64	64
Area/Chan. (mm^2)	0.09	0.1	0.5	0.025	0.09
Gain (dB)	54-60	68-78	41-61	N/R	51
Noise (μV_{rms})	5.1	9.3	5.23	0.57	4.2
f_{L3dB} (Hz)	1	0.1	0.5	1	1
f_{H3dB} (Hz)	5k	8k	7k	500	5k
Chopper	64	0	0	64	64
Amp. Count					
Signal Proc.	YES	NO	YES	NO	YES
closed-loop	YES	NO	YES	NO	YES
Detection- algorithm	Amp/ ϕ	-	Entropy	-	Synchrony
closed-loop	YES	NO	YES	NO	YES
Stimulation					
# Stim. chan.	64	0	1	-	64
Current Range	≤ 1.2 mA	-	$\leq 30\mu$	-	10 μ A-1mA
Wireless power	NO	YES	YES	YES	YES
Rec. Coil	-	One-Layer	Wire-	μ fabricated	8-Layer
type		Rigid PCB	Wound	Antenna	Flex PCB
Size	-	Diam: 3 cm	N/R	Diam: 6.5mm	2cmx2cm
# of Turns	-	2	N/R	N/R	104
Inductance (μH)	-	0.41	N/R	N/R	176
Coil Separation	-	12 cm	N/R	N/R	12 cm
Power Transfer	-	N/R	N/R	N/R	40%
Efficiency					
Frequency	-	13.56 MHz	13.56MHz	300MHz	1.5 MHz
# of Voltage	-	N/R	N/R	1	10
Levels	-	N/R	3		
Wireless Comm.	YES	YES	YES	YES	YES
Modulation	UWB	FSK	OOK	N/R	Band1: UWB Band2: UWB Band3: FSK
Frequency	0-1 GHz	915 MHz	403 MHz	300 MHz	Band1: 3.1-10.6 GHz Band2: ≤ 1 GHz Band3: 916.4 MHz
In-vivo	YES	NO	YES	YES	YES
Sensitivity	N/R	-	92%	N/R	88-96%
Selectivity	N/R	-	N/R	N/R	89-97%

-: Not Applicable

N/R: Not Reported

* Without and With FSK Transmitter

model. It demonstrates early seizure detection and abortion in freely moving rodents.

REFERENCES

- [1] A. Berenyi, et al., "Closed-Loop Control of Epilepsy by Transcranial Electrical Stimulation," *Science*, vol. 337, no. 6095, pp. 735-737, Aug. 2012.
- [2] W.-M. Chen, et al., "A fully integrated 8-channel closed-loop neural-prosthetic SoC for real-time epileptic seizure control," *ISSCC 2013*, pp. 286-287.
- [3] K. Abdelhalim, et al., "64-channel UWB wireless neural vector analyzer SOC with a closed-loop phase synchrony-triggered neurostimulator," *JSSC* vol. 48, no. 10, pp. 2494-2510, 2013.
- [4] K. Abdelhalim, et al., "915-MHz FSK/OOK Wireless Neural Recording SoC With 64 Mixed-Signal FIR Filters," *JSSC*, no. 99, pp. 1-16, 2013.
- [5] S. B. Lee, et al., "An inductively powered scalable 32-channel wireless neural recording system-on-a-chip for neuroscience applications," *TBioCAS*, vol. 4, no. 6, pp. 360-371, 2010.
- [6] Xu, Jiawei, et al. "A 60nV/ $\sqrt{\text{Hz}}$ 15-channel digital active electrode system for portable biopotential signal acquisition." *ISSCC 2014*, pp. 424-425.
- [7] W. Biederman, et al. "A fully-integrated, miniaturized (0.125 mm^2) 10.5 w wireless neural sensor," *JSSC*, vol. 48, no. 4, pp. 960-970, Apr. 2013.
- [8] Muller, Rikky, et al., "A miniaturized 64-channel 225W wireless electrocorticographic neural sensor." *ISSCC 2014*, pp. 412-413.